M. Salman Naeem[1], Naseer Ahmad[1], Zafar Javed[1*], Abdul Jabbar[1], Ateeq ur Rehman[1], Muhammad Zubair[1], Syed Qummer Zia Gilani[1], Zuhaib Ahmad[1], Mehmet Karahan[2**]

# Multi-Response Optimisation for the Development of an Activated Carbon Web as Interlining for Higher Electrical Conductivity and EMI Shielding Using Grey Relational Analysis

**DOI:** 10.5604/01.3001.0014.5046

[1] National Textile University, Faculty of Engineering, Faisalabad, 37610, Pakistan,
* e-mail: Zafar@ntu.edu.pk

[2] Uludağ University, Vocational School of Technical Sciences, Görükle-Bursa, Turkey
** e-mail: mkarahan@uludag.edu.tr

**Abstract**
*This paper presents a simple and novel method of producing an activated carbon (AC) non-woven web from acrylic waste derived from discarded bathmats converted into a nonwoven web by a carding and needle punching machine. After stabilisation at lower temperature, carbonisation of the stabilised web was performed in a muffle furnace. The carbonisation temperature, the holding time of the activated carbon web at the final temperature, the heating rate to reach the final carbonisation temperature and the number of steps adopted for developing the carbon web were optimised using the grey relational analysis (GRA) approach to get optimum responses of the surface area of the web, electrical conductivity and electromagnetic shielding. The results demonstrated a large improvement in electrical conductivity as surface resistivity decreased from 134.21 Ω.mm to 0.28 Ω.mm, and the corresponding electromagnetic shielding increased to 82.63 dB when the temperature of the carbonisation, the holding time and number of steps were increased. The surface area in the AC web was increased from 73 $m^2g^{-1}$ to 210 $m^2g^{-1}$ with an increase in the carbonisation temperature, the holding time and number of steps to reach the final temperature. The optimisation technique used in this work could be successfully used in cost and error reduction while producing an AC web. The optimised AC web was characterised by Brunauer, Emmett and Teller (BET), X-ray diffraction characterisation and elemental analysis (EDX) in order to determine changes in its structure, surface area, degree of crystallinity, inter-layer spacing and proportion of different elements. The AC web developed can be effectively employed as interlining in apparels because of its flexibility and eco-friendly electromagnetic shielding, as it works on the principle of the absorption, reflections and internal reflections of electromagnetic radiations.*

**Key words:** *activated carbon, stabilisation, carbonisation, electromagnetic shielding.*

## Introduction

Nowadays, research on conductive fabrics having good electromagnetic shielding is becoming popular because of their enormous applications in different fields such as medicine, the military, smart textiles and electromagnetic shielding. In the present age of communication where humans and devices are surrounded with other different instruments, the importance of electromagnetic shielding has been magnified [1, 2]. Although it is not new that humans are facing electromagnetic radiations but in this era of technological advancements coupled with excessive use of electronic devices, scientists and researchers are pushed to divert their attention towards this evolving issue [3].

Electronic instruments emit electromagnetic radiations which are not only dangerous for humans but also cause disturbance to the smooth working of other electronic devices [4]. Electromagnetic shielding materials block these radiations through different mechanisms, in which the reflection of rays from the surface of the material, and the absorption of radiations and internal reflections of electromagnetic rays within the shielding material play an important role [5, 6]. Highly conductive materials such as metals work as electromagnetic shielding materials by reflecting electromagnetic radiations; however, these have the limitations of high density, corrosiveness and lack of flexibility [7]. Currently, researchers are trying to use carbon-based materials as fillers on different textile structures to get higher electromagnetic shielding application because of their large surface area and higher electrical conductivity [8]. Neruda used conductive yarns in woven fabrics and found that electromagnetic shielding effectiveness up to 25-50 dB was achieved; however, these kinds of fabrics were accompanied with a stiff structure [9]. In his study, Cao used carbon nanotubes with ferroferic oxide to obtain better magnetic and electromagnetic shielding properties [10]. M. Tian deposited a graphene layer on a cotton fabric substrate to get a conductive and flexible woven structure. Graphene deposited cotton fabric gave a high electromagnetic shielding value of 30.04 dB with good flexibility and drape [8]. Li concluded that a composite structure of graphene and ultrathin polyamide foam gave a 24 dB shielding efficiency. He further revealed that shielding effectiveness in the same material was increased from 24 dB to 51 dB as the thickness of the material was increased from 24 μm to 73 μm [11]. However, the foam ability and porosity of conductive foams are adversely affected as the proportion of conductive particles is increased. Much of the work on electromagnetic shielding is focused on the use of conductive fillers, metallic yarns in woven fabrics, the coating of conductive polymers. and carbon-based materials. However, there is a need to explore a nonwoven structure comprising conductive fibres.

***Table 1.*** *Process parameters with their levels.*

| Factor | Code | Unit | Levels | | |
|---|---|---|---|---|---|
| | | | 1 | 2 | 3 |
| Carbonization Temp. (CT) | A | °C | 800 | 1000 | 1200 |
| Holding Temp. (HT) | B | °C | 0 | 30 | 60 |
| Heating Rate (HR) | C | °C | 150 | 350 | 450 |
| Number of Steps (NOS) | D | – | 1 | 2 | 3 |

Activated carbon fibre (ACF) is a porous fibre with a diameter of around 10 µm. It is more convenient to optimizes the surface area of ACF through controlling the pore diameter and pore size, which in turn has a positive impact on electrical conductivity and electromagnetic shielding as compared to other forms of activated carbon. Different researchers have adopted different raw materials, carbonisation techniques like physical or chemical activation and metal impregnation for attaining the desired surface area and porosity. Miguel developed AC from waste rubber tyres at a temperature of 700-950 °C and got a surface area in the range of 545-789 $m^2/g$. The surface area and porosity can be increased by using the chemical activation method, but this is not favorable for developing an AC web as it gives a more porous and fragile structure. Laila produced AC with a high surface area of 827 $m^2/g$ using a carbonisation temperature of 700 °C through the chemical activation method. However, there is an inverse trend between electrical conductivity and the surface area of activated carbon [12]. Research is underway to find alternative and inexpensive materials not only to increase the yield of the resulting AC but also to achieve better conductivity and electromagnetic shielding. Polyacrylonitrile [13-15], Polyacrylamides [16], phenolic resins [17, 18], pitch and cellulosic fibres [19] are the most often used as raw material for the formation of AC.

Much work has already been done on the development of porous morphology with good electromagnetic shielding ability. However, the development of flexible material having porous morphology with good electrical conductivity and electromagnetic shielding at an economical price is still a problem. This work gives an effective and novel technique for producing an AC web from a needle punched nonwoven acrylic web through stabilisation and carbonisation at higher temperature. Three levels of each factor including the carbonisation temperature (800, 1000 and 1200 °C), heating rate (150, 300 and 450 °C $hr^{-1}$), holding time (0, 30 and 60 minutes) and number of steps (1, 2 and 3 step approach) for carbonisation, were selected to analyse their impact on the surface resistivity, surface area and electromagnetic shielding of the AC web. The variables selected were optimised using the Taguchi technique of GRA to obtain the best possible results of surface resistivity, electrical conductivity and electromagnetic shielding.

## Materials and methods

### Material

Acrylic waste was sourced from Grund Industries, Czech Republic, in the form of discarded bathmats as raw material for the formation of an AC web. Acrylic is a Polyacrylonitrile (PAN) based co-monomer which contains around 85 to 90% of acrylonitrile monomer. The acrylic fibres possess 2.4% wet shrinkage and 43% breaking elongation. The tenacity and fineness of these fibres were found to be 23.84 cN/tex and 117 tex, respectively.

### Design of experiment

The Taguchi technique is a statistical technique employed for improving the quality of manufactured products. This technique compares the mean of a process with noise (variations) termed as the signal-to-noise ratio (S/N). Single response optimisation is performed using the Taguchi technique. However, grey relational analysis along with the Taguchi method gave the best solution of optimisation for multi-response optimisation. Taguchi's methodology compares the magnitude of the mean (signal) of a process to the variation (noise), termed as the signal-to-noise (S/N) ratio. The Taguchi method is used only for optimisation of a single response. For multi-response optimization, Taguchi methodology coupled with grey relational analysis (GRA) is the best solution for simultaneous optimisation of multiple responses. Taguchi-based GRA is applied to obtain the optimum settings of process parameters subject to the simultaneous optimisation of multiple responses. In the Taguchi method, S/N ratios are computed as nominal-the-better, smaller-the-better, and higher-the-better. The S/N ratio is the ratio of sensitivity to variability and is used to examine conceptually the effect of control factors for the function of product and process. The noise ratio is used in terms of the magnitude of voice in the communication industry and is expressed in decibels (dB), and the normalised SN ratio is the unit-free data sequence. The corresponding S/N ratios are given below:

$$S/N(nominal-the-better) = \\ = -10log|(\bar{y}-T)^2+s^2| \quad (1)$$

Where, $\bar{y}$: mean value, $T$: target value, $n$: number of tests, $s$: standard deviation of sample,

$$s=\sqrt{\frac{\sum_{i=1}^{n}(y_i-\bar{y})^2}{n-1}}$$

$$S/N\ (smaller-the-better) = \\ = -10log(\bar{y}^2+s^2) = -10log\left(\frac{1}{n}\sum y_i^2\right) \quad (2)$$

$$S/N\ (higher-the-better) = \\ = -10log\left(\frac{1}{n}\sum\frac{1}{y_i^2}\right) \quad (3)$$

In this study, smaller-the-better ***Equation (1)*** and higher-the-better ***Equation (3)*** S/N ratios were taken into consideration to minimise surface resistivity and maximizes the surface area and electromagnetic shielding. An orthogonal array $L_9$ was used, which required only nine experiments. Factors whose levels were considered in this study are given in ***Table 1***. In this study, we used statistical and computational software including Minitab 18, R 4.0.0, Design Expert v11 and Microsoft Excel 13 to design experiments as well as for computation, and optimisation of statistical results.

In the present study, three responses (electrical conductivity, electromagnetic shielding and surface area of the web) were taken to optimise simultaneously, and grey relational analysis (GRA) was employed to optimise the responses. The methodology of GRA is given in detail in an earlier study [20].

### Preparation of a carbon web from acrylic waste

Acrylic fibres were manually removed from bathmats. The fibres were then washed with distilled water to remove impurities and dust from their surface. The washed fibres were then dried in an oven at 100 °C. Next, the fibres were card-

ed and then needle punched on a needle punching machine, where the speed of feeding the acrylic web was maintained at 0.5 metres per second. The depth of needle penetration was 5 mm at a speed of 200 strokes/minute. The acrylic web produced had a density of 2.77 g/cm$^3$, with a thickness of 12.2 mm. A fixed size of non-woven acrylic web: 25 cm (wide) and 25 cm (long) was cut and transferred to a high temperature furnace for stabilisation and carbonisation. A schematic diagram of the formation of activated carbon can be seen in ***Figure 1***.

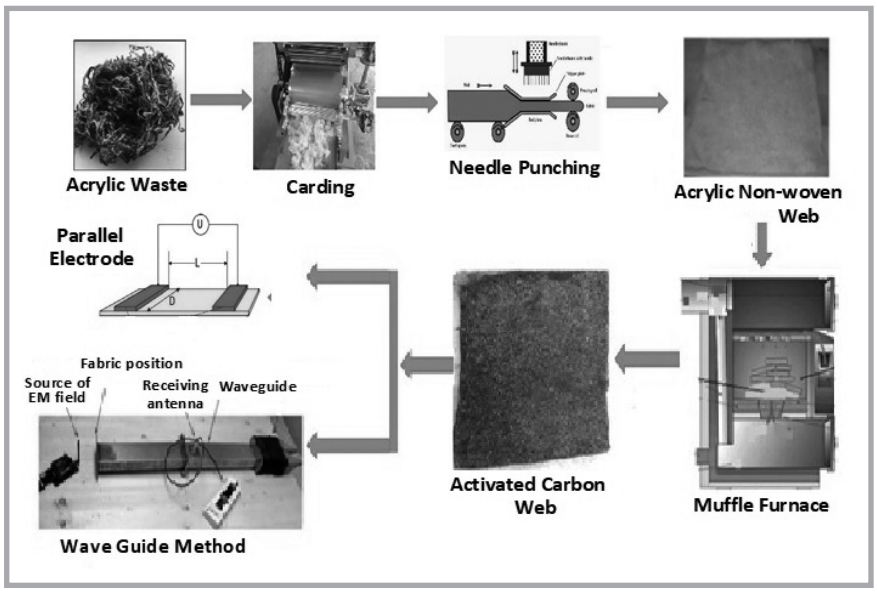


***Figure 1.*** *Schematic diagram of the formation of an AC web.*

**Characterisation of an AC web**

Physical characteristics such as flexibility, yield and shrinkage of AC webs prepared with different heating rates, holding times, number of steps and carbonization temperatures were determined. The flexibility of AC webs was determined using the cantilever bending principle following the ASTM D1388 standard. This method determines flexibility through determination of the bending length under its own weight. The shrinkage was determined by measuring changes in the dimensions of the acrylic web before stabilisation and after carbonisation at different temperatures. Finally, the yield of the AC webs prepared was determined using ***Equation (4)***.

$$Yield\ (\%) = = \frac{Weight\ of\ activated\ carbon\ web}{Weight\ of\ acrylic\ web} \times 100 \quad (4)$$

***X-Ray Diffraction (XRD) analysis***

X-ray diffraction analysis was conducted on a Malvern PAN analytical Xpert powder machine with a copper anode source (0.15406 nm). The XRD analysis helped to determine the inter planer distance among the layers of carbon basal planes, for wich the famous Bragg's ***Equation (5)*** was used:

$$2d \sin\theta = n\lambda \quad (5)$$

This technique also helped to determine the change in the presence of amorphous regions and the increase in crystalline regions in the AC prepared web, which can be calculated using ***Equation (6)*** [21].

$$I_c = 1 - \frac{I_1}{I_2} \quad (6)$$

Here, $I_c$ represents crystallinity, expressed in %; $I_1$ corresponds to the intensity at the lowest point, and $I_2$ shows the intensity at the highest point in the XRD spectrum.

***EDX analysis of AC web***

EDX technique was employed to investigate presence of different elements (carbon, nitrogen, sulfur, hydrogen, oxygen etc.) and their corresponding concentrations in AC web. This analysis was conducted on the Oxford instrument.

***BET analysis of AC web***

The development of the surface area on the AC web was determined using Brunauer Emmett and Teller (BET) analysis. This analysis was performed on an Autosorb iQ, Quantachrome. In this method adsorption and desorption curves of nitrogen helped to investigate the surface area developed on the AC web. The range of relative pressure for nitrogen ($P/P_o$) was maintained between 0.02-1.

***Electrical conductivity***

The parallel electrode technique was used to determine surface resistivity by following ASTM D-257 at 40% relative humidity and 25 °C temperature. The resistivity was determined by applying a voltage difference of 1 volt across the electrodes. The surface resistivity was established after 15 ± 1 s using the following ***Equation (7)***.

$$\rho = R \times \frac{D}{L} \quad (7)$$

Where, ρ – surface resisivity, ohm, $D$ – width of parallel electrodes, cm, R – surface resistance, ohm, L – space between parallel electrodes, cm.

***Electromagnetic shielding effectiveness***

The waveguide method was used to determine the electromagnetic shielding of the AC web. This technique was used to evaluate the electromagnetic shielding effectiveness at 2.45 GHz following ***Equation (8)***. This method utilised a hollow tube with electrically conductive walls. The carbon web was placed at the entrance of the tube, contained a receiving antenna.

$$SE = 10\ \log\frac{P_t}{P_i} \quad (8)$$

Where, $SE$ denotes shielding effectiveness, measured in dB; $P_i$ – corresponds to the power intensity without the sample, W/m$^2$, and $P_t$ – shows the power intensity in the presence of the sample, W/m$^2$.

## Results and discussion

Activated carbon fibres have gained significant attention over the last decade due to their extraordinary adsorption characteristics towards heavy metals, different poisonous gases, dyes and other hazardous chemicals [22]. Besides adsorption characteristics, AC has very good electrical conductivity and electromagnetic shielding properties, which decrease with increasing the surface area [23]. Serious efforts are being made to develop a nonwoven AC web with optimised parameters to get a good surface area, electrical conductivity and electromagnetic shielding. For this purpose, initially the acrylic web was stabilised at a lower temperature, and then carbonised at a higher temperature to obtain good conductivity and electromagnetic shielding. Different

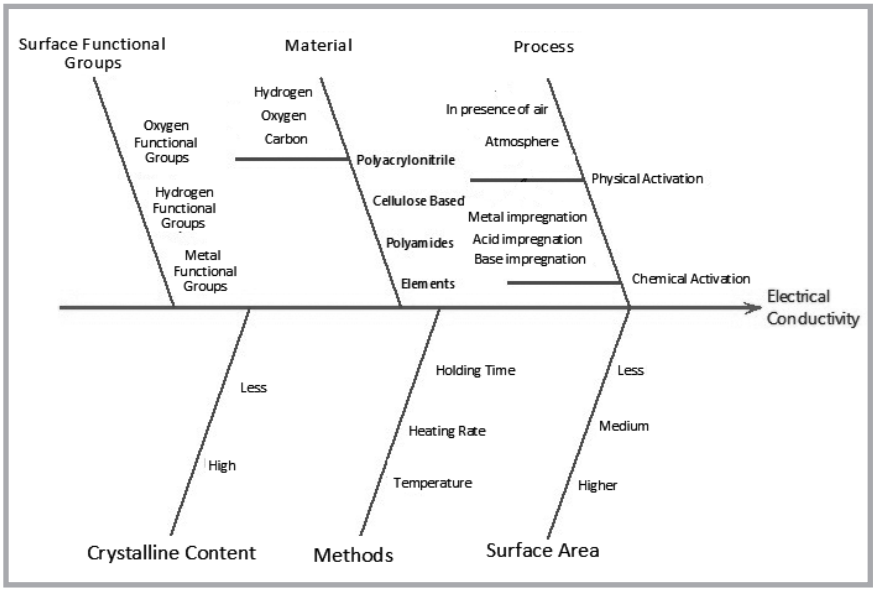


***Figure 2.*** *Cause & effect diagram of electrical conductivity.*

characterisation techniques were employed to investigate the physical morphology and chemical characteristics of the AC web.

## Cause and effect

The different factors affecting the electrical conductivity of the AC web can be seen from the cause and effect diagram (***Figure 2***) [12].

The electrical conductivity depends on the physical activation processes (inert atmosphere using nitrogen or argon, presence of air), chemical activation (acid activation, base activation, metal impregnation), surface area, type of materials (polyacrylonitrile, cellulosics, polyamides), carbonisation temperature, heating rate, holding time, number of steps and surface functional groups [24]. In addition, crystalline contents and elements (carbon, oxygen, hydrogen) also affect the electrical conductivity process [12].

## Taguchi method

In the present study, a Taguchi based orthogonal array $L_9$ was applied which required only nine experimental runs with three replications. Results of each experimental run and nine experiments with three replicates were obtained. The factors and their levels considered in this study are shown in ***Table 1***, and the orthogonal array L9 with factors and responses along with the standard deviation are given in ***Table 2***. The confidence interval (CI) is a parameter estimation technique, 95% CI is the most commonly used, which implies that an interval estimate of 95% of samples will contain the population parameter value. As far as the specific surface area was concerned, it slightly increased at 1200 °C due to the more arrangement of carbon planes and removal of non-carbon elements. However, a significant increase in electrical conductivity and electromagnetic shielding was observed when increasing the carbonisation temperature as it caused a more parallel arrangement of carbon chains and a reduction in inter layer spacing, which brought about a condensed structure of carbon with more availability of hoping electrons.

***Table 2.*** *Taguchi design of experiment with factors and responses.*

| Sr. No. | Factors | | | | Responses | | |
|---|---|---|---|---|---|---|---|
| | Carbonisation temp, CT, °C | Holding temp., HT, °C | Heating rate, HR, °C | NOS | Surface area, $m^2/g$ | Surface resistivity, Ω.mm | Electromagnetic shielding, dB |
| 1 | 800 | 0 | 150 | 1 | 73 ± 2.53 | 134.21 ± 1.63 | 2.36 ± 0.24 |
| 2 | 800 | 30 | 300 | 2 | 103 ± 3.36 | 867.82 ± 1.63 | 3.6 ± 0.35 |
| 3 | 800 | 60 | 450 | 3 | 51.67 ± 6.18 | 305.96 ± 5.09 | 4.93 ± 0.63 |
| 4 | 1000 | 0 | 300 | 3 | 160 ± 6.48 | 7.64 ± 0.48 | 73.5 ± 0.40 |
| 5 | 1000 | 30 | 450 | 1 | 65 ± 2.16 | 3.9 ± 0.01 | 75.93 ± 0.77 |
| 6 | 1000 | 60 | 150 | 2 | 124.33 ± 9.28 | 1.47 ± 0.07 | 76.46 ± 0.38 |
| 7 | 1200 | 0 | 450 | 2 | 110 ± 2.82 | 1.17 ± 0.05 | 80.13 ± 0.12 |
| 8 | 1200 | 30 | 150 | 3 | 188 ± 3.74 | 0.52 ± 0.10 | 81.34 ± 0.04 |
| 9 | 1200 | 60 | 300 | 1 | 210 ± 9.90 | 0.28 ± 0.03 | 82.63 ± 0.97 |

***Table 3.*** *Taguchi and GRA based computed parameters.*

| Exp. No. | S/N ratio | | | Standardised S/N ratio | | | Quality loss function values | | | Grey relational coefficient | | | Grey grade |
|---|---|---|---|---|---|---|---|---|---|---|---|---|---|
| | Y1 | Y2 | Y3 | $Y_1$ | $Y_2$ | $Y_3$ | $\Delta Y_1$ | $\Delta Y_2$ | $\Delta Y_3$ | $GCY_1$ | $GCY_2$ | $GCY_3$ | $G_i$ |
| 1 | 37.25 | -42.56 | 7.34 | 0.26 | 0.77 | 0.00 | 0.742 | 0.232 | 1.000 | 0.574 | 0.811 | 0.500 | 0.629 |
| 2 | 40.24 | -58.77 | 10.99 | 0.50 | 1.00 | 0.12 | 0.499 | 0.000 | 0.883 | 0.667 | 1.000 | 0.531 | 0.733 |
| 3 | 34.06 | -49.71 | 13.66 | 0.00 | 0.87 | 0.20 | 1.000 | 0.130 | 0.796 | 0.500 | 0.885 | 0.557 | 0.647 |
| 4 | 44.06 | -17.68 | 37.33 | 0.81 | 0.41 | 0.97 | 0.190 | 0.589 | 0.033 | 0.840 | 0.629 | 0.968 | 0.813 |
| 5 | 36.24 | -11.83 | 37.61 | 0.18 | 0.33 | 0.98 | 0.823 | 0.673 | 0.024 | 0.549 | 0.598 | 0.977 | 0.708 |
| 6 | 41.82 | -3.36 | 37.67 | 0.63 | 0.21 | 0.98 | 0.372 | 0.794 | 0.022 | 0.729 | 0.557 | 0.979 | 0.755 |
| 7 | 40.82 | -1.40 | 38.08 | 0.55 | 0.18 | 0.99 | 0.453 | 0.823 | 0.009 | 0.688 | 0.549 | 0.992 | 0.743 |
| 8 | 45.48 | 5.44 | 38.21 | 0.92 | 0.08 | 1.00 | 0.076 | 0.921 | 0.004 | 0.930 | 0.521 | 0.996 | 0.815 |
| 9 | 46.41 | 10.99 | 38.34 | 1.00 | 0.00 | 1.00 | 0.000 | 1.000 | 0.000 | 1.000 | 0.500 | 1.000 | 0.833 |

**Optimisation of parameters through GRA**

In GRA, experimental response values of the three responses that are surface area, surface resistivity and electromagnetic shielding were taken. Grey relation grades (GRGs) were evaluated by the following the steps of GRA methodology, as discussed earlier.

**Step 1:** Each response was converted into S/N ratios, which are given in ***Table 3***. The S/N ratios are expressed as higher-the-better in the case of the surface area and electromagnetic shielding, while in the case of surface resistivity, lower-the-better is used. In other words, higher surface area and electromagnetic shielding are required along with retention or improvement in another feature of the AC web of the treated sample.

**Step 2:** For computation of the relative quality characteristics of responses and to acquire the objectives of GRGs, standardised S/N ratios of multiple responses were computed. Normalised S/N ratios of various multiple responses were also computed. A normalised S/N ratio near to one is considered as ideal. Larger S/N ratios, 46.41 and 38.34, noted for the surface area and electromagnetic shielding, respectively, correspond to better performance (***Table 2***).

**Step 3:** After computing the standardised S/N ratios of each response and by using the equation: Quality Loss $\Delta = |Z_o - Z_{ij}|$, the quality characteristic of each response was judged by computing the quality loss function, which is given in ***Table 3***.

**Step 4:** In this step, based on the quality loss function and quality loss values, the grey relational coefficients (GCs) of each response were calculated. The resultant values of GCs are also given in ***Table 3***.

**Step 5:** Simultaneous optimisation of the quality characteristics of multiple responses are expressed as a single response GRG, and the GRG in this step was computed for each response by taking the arithmetic mean of the GCs of each response (***Table 3***).

**Step 6:** In this step, the main effects on grey grades were computed by taking the mean value of the GRG values which gave the prediction of optimum levels of the factors for the simultaneous optimisation engineering problem. In this way, the multi-response in converted into a single response optimisation problem. The main effects on grey grades are expressed in ***Table 3***.

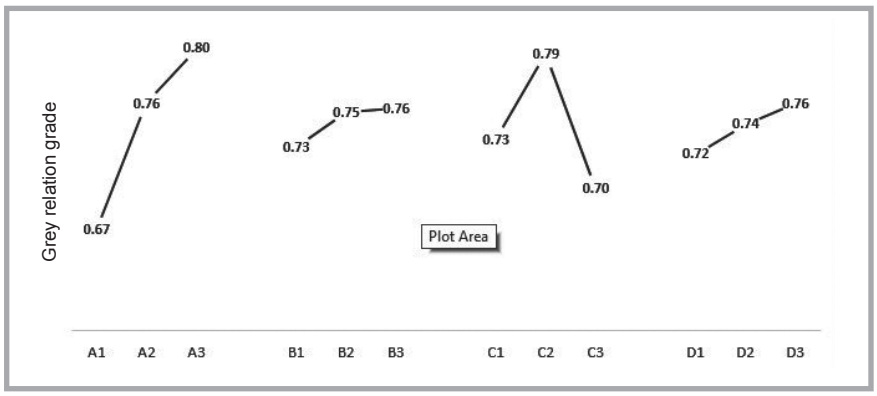


***Figure 3.*** *Factor effects on the grey grade.*

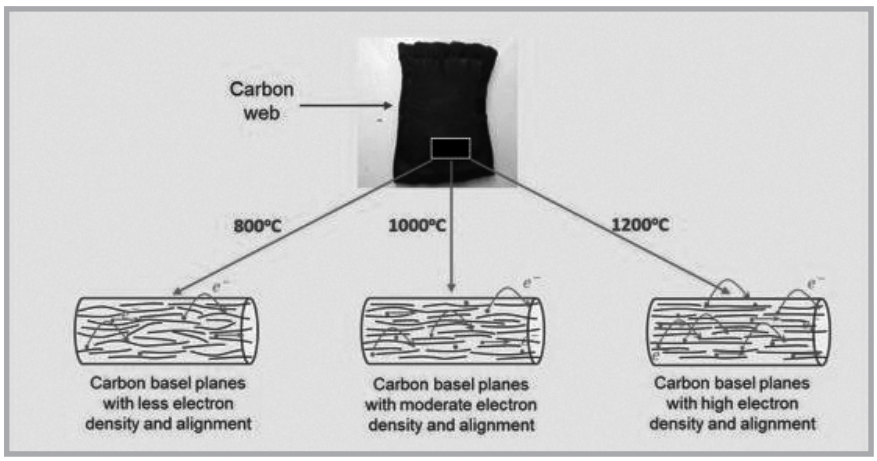


***Figure 4.*** *Mechanism of rise on electrical conductivity in AC webs.*

The mean of the GRG values was obtained and can be seen in ***Table 4***, and a graph of the main effects of GRG can be observed in ***Figure 3***, which showed the optimum process parameters for obtaining multiple responses. ***Figure 3*** explains the effect of electrical conductivity with different factors and their levels. The higher GRG value implies better multiple quality responses and shows a ratio of S/N near to unity.

**Step 7:** From step 6, we obtained optimum settings of process parameters (viz., carbonisation temperature, holding temperature and heating rate) as $\mathbf{A_3B_3C_2D_3}$ i.e., a carbonisation temperature of 1200 °C, a holding temperature of 60 °C, and a heating rate of 300 °C, with a three step approach, as shown in ***Table 4***.

An AC web was prepared at these optimum settings of process parameters, and responses were analysed through different characterisation techniques. The AC web prepared at the prescribed settings showed different behaviour in terms of yield, flexibility and shrinkage. A higher reduction in the yield of the AC web resulted when the carbonisation temperature was increased to 1200 °C because the AC web suffered a higher degree of carbonisation, which resulted in more elimination of disorganised carbon and non-carbon atoms from carbon planes. At a higher heating rate the AC web turned into a fused structure due to the abrupt rise in the carbonisation tempera-

***Table 4.*** *Main effects on grey grades.*

| Factors | 1 | 2 | 3 | Max – Min |
|---|---|---|---|---|
| A: CT | 0.670 | 0.758 | 0.797 | 0.128 |
| B: HT | 0.728 | 0.752 | 0.755 | 0.024 |
| C: HR | 0.733 | 0.793 | 0.699 | 0.094 |
| D: NOS | 0.723 | 0.744 | 0.758 | 0.035 |

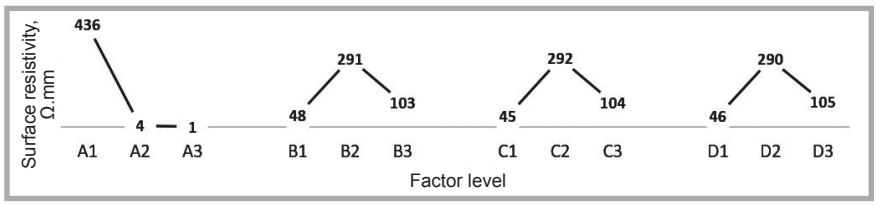


***Figure 5.*** *Factors effecting surface resistivity (Ω.mm) of AC web.*

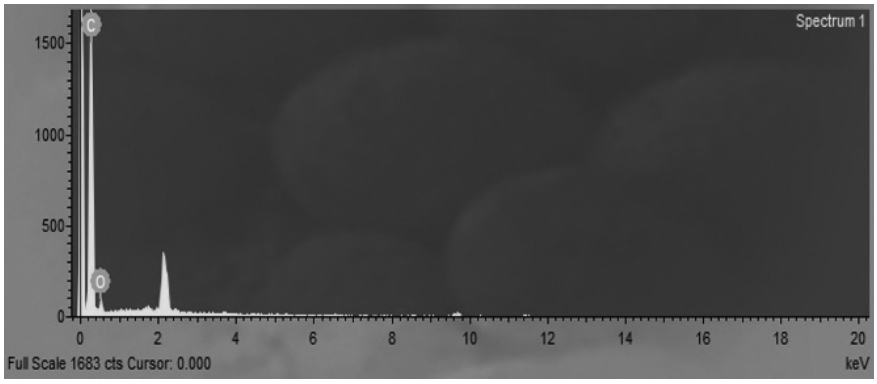


***Figure 6.*** *EDX pattern of AC web.*

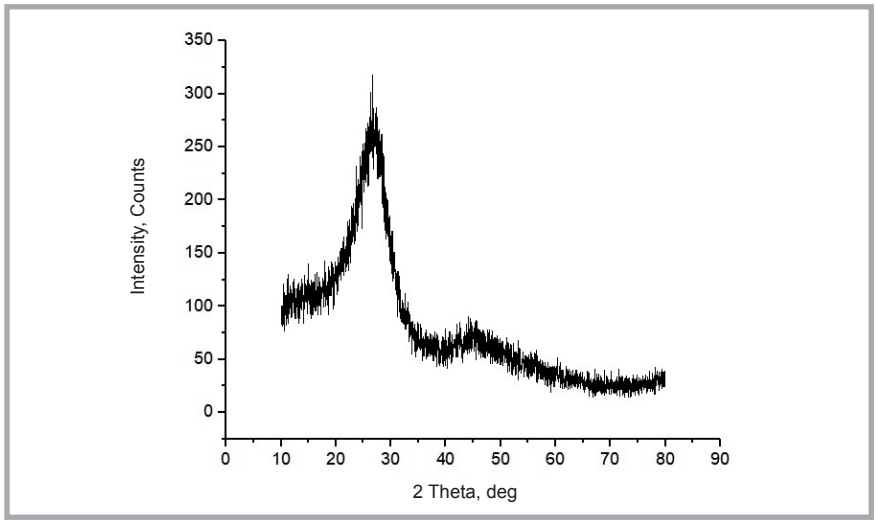


***Figure 7.*** *X-ray diffraction analysis pattern of AC web.*

ture; however, the AC carbon web faced with higher carbonisation temperature for a longer time at a slow heating rate caused more shrinkage and a reduction in flexibility. When the holding time at the final carbonisation temperature was increased, it resulted in higher carbonisation as well as an increase in graphitisation, thus leading to a compact structure.

**Characterisation of electrical conductivity**

Higher electrical conductivity in the AC web was achieved by increasing the carbonisation temperature to 1200 °C with a 60 minute holding time at 300 °C $hr^{-1}$ and using the three step approach. The slower heating rate also resulted in higher conductivity due to the more prolonged exposure of the AC web at a higher carbonisation temperature. Although a slower heating rate caused a higher degree of crystallinity, it adversely affected the yield and flexibility of the carbon web. When the temperature during the carbonization process was increased to 1200 °C, the surface resistivity decreased due to more graphitisation and the reduction in inter planar distances among the carbon basal planes [25]. The mechanism of the rise in electrical conductivity with the rise of temperature is explained in ***Figure 4***.

***Table 6.*** *Different carbon-based materials with different EM shielding capabilities.*

| Substrate | Carbon materials | EM SE (dB) |
|---|---|---|
| Cotton | Multi walled carbon nanotubes | 9.0 [28] |
| Polyester | Nano carbon black | 7.7 [29] |
| Non-woven | Carbon nanotube | 15-40 [30] |
| Cotton | Carbon black | 31.39 [31] |
| Acrylic | AC web | 82.63 (This work) |

***Table 5.*** *Characteristics of XRD pattern.*

| | |
|---|---|
| Degree of crystallinity | 94.1% |
| Crystallite size | 23.5 Angstrom |
| d-Spacing | 45.2 nm |

It can be seen from ***Figure 4*** that as the temperature during carbonisation was increased, it resulted in a more compact structure, which caused a saturation of electron clouds and provided an easier path for the flow of electrons. This easy path for the flow of electrons caused higher electrical conductivity at a higher temperature. At a higher carbonisation temperature with a 60 minute holding time, non-carbon elements like hydrogen, sulfur and nitrogen along with electron accepting functional groups were eliminated, leaving behind carbon chains which became more aligned and parallel to each other, as shown in ***Figure 5*** [26]. At higher temperature, the increase in the holding time and number of steps gave better conductivity because of improved stabilisation and higher carbonisation.

The electrical resistivity of the AC web at the prescribed optimum settings was found to be 0.28 Ωmm. EDX analysis of the AC web showed 87.70% carbon, while the oxygen content was 12.30%, as presented in ***Figure 6***.

XRD analysis results are given in ***Table 5***, and the pattern is presented in ***Figure 7***, which shows a peak at around 26 degrees, confirming lattice planes of graphite structure.

**Characterisation of electromagnetic shielding**

Results of the electromagnetic shielding of the AC web prepared at different settings are given in ***Table 2***, showing that an increase in temperature during

carbonisation resulted in a reduction in surface resistivity and rise in electromagnetic shielding [23, 27]. In ***Table 6*** electromagnetic shielding values of different carbon-based materials can be seen.

Although AC webs at a lower carbonisation temperature were thicker as compared to those prepared at a higher carbonisation temperature the resistivity of the shielding material and compact structure of the web are more important for obtaining good electromagnetic shielding. The web prepared with a high temperature and holding time gave more conductivity, higher compactness and a more dense structure of carbon basal planes [23]. which not only increased the absorption of electromagnetic radiations but also caused higher internal multiple reflections of these radiations. The mechanism of the rise in electromagnetic shielding in different AC webs is shown in ***Figure 8***.

By increasing the carbonisation temperature, denser electron clouds were developed in the web due to higher conductivity. These electron clouds caused more absorption of electromagnetic radiations, which ultimately resulted in higher electromagnetic shielding at higher temperature. As far as the heating rate is concerned, it did not cause a sufficient rise in electromagnetic shielding; however, a too high heating rate did cause a sudden rise in temperature, which resulted in a more fused and brittle structure of the carbon web. In the case of a low heating rate, the electromagnetic shielding was also not much affected, but it did result in a higher reduction in the yield of the web. The impact of the heating rate, holding time, carbonisation temperature and number of steps on electromagnetic shielding can be seen in ***Figure 9***.

In the three step approach, although shielding was not changed much as compared to the single and two step approaches, proper stabilisation of the web was achieved, which contributed to a positive impact on the morphology of the AC web in terms of its flexibility. The optimised settings of selected factors showed an electromagnetic shielding of 82.63 dB due to the removal of impurities other than oxygen, which was confirmed from the EDX pattern. The higher shielding at the prescribed optimum settings was due to the reduction in inter layer spacing, which produced a compact

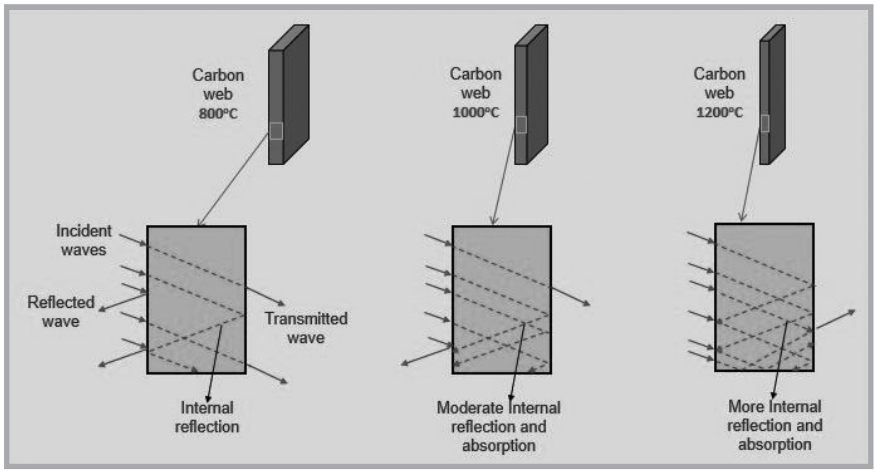


***Figure 8.*** *Mechanism of the rise in electromagnetic shielding effectiveness in AC webs.*

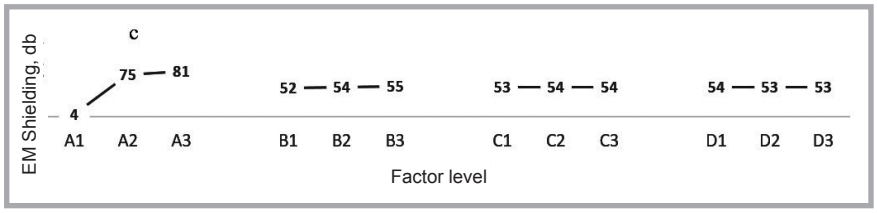


***Figure 9.*** *Factors effecting electromagnetic shielding application of AC web.*

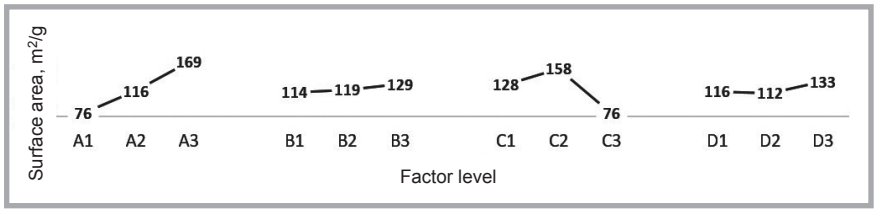


***Figure 10.*** *Factors effecting specific surface area of AC web.*

structure of the web. The compactness of the web enabled the availability of not only hoping electrons but also the easy movement of electrons between chains, which had a positive impact on the absorption of electromagnetic radiations [32, 33], as shown in ***Figure 8***.

**Characterisation of surface area**

Besides its granular and powder form, activated carbon fibre (ACF) also exists, being a porous carbon material fibre. It has different diameters with a narrow pore size and varying surface area. In the fibre form of activated carbon, the pore length and pore diameter are more easily controlled when compared with the granular and powder form. The electrical properties of ACF vary widely and depend on the structure of fibres. An increase in the surface area instigated a negative impact on surface resistivity and electromagnetic shielding [12]. When the carbonisation temperature was gradually increased to the highest temperature, it resulted in a random arrangement and rearrangement of carbon basal planes and micro crystallites. Furthermore, at higher temperature, the removal of disorganised carbon and the elimination of elements like nitrogen, sulfur, hydrogen etc. created pores and voids in the structure of AC fibres [34]. When the holding time was increased at high temperature, it increased the compactness of the web and its surface area due to the removal of disorganised carbon from the edges of the carbon chain. When the heating rate was slow, it took more time to reach the final carbonisation temperature, which resulted in the formation of char that filled the pores of fibres, hence contributing to a reduction in the surface area, as shown in ***Figure 10***. On the other hand, when the heating rate was too high, it resulted in a fused structure of the web, which was also the reason for the reduction in its surface area [34]. The one step approach was not favorable to get a higher surface area since stabilisation was not performed and the resulting web at high temperature turned

into a brittle structure, thus losing its flexibility.

It is preferable to obtain less surface area to achieve good electrical conductivity and electromagnetic shielding. The AC web at optimised settings showed a surface area of 210 $m^2/g$. In the optimised AC web, although the surface area was increased slightly, less surface area was not the only reason for greater conductivity and electromagnetic shielding, as other factors like d-spacing, degree of crystallinity, graphitisation, crystallite size and carbon content also had a positive impact on getting the desired results.

## Conclusions

This work showed the successful transformation of acrylic waste into an acrylic web which was subsequently transformed into an AC web using a high temperature muffle furnace. The morphology and structural characteristics of the AC web drastically changed by varying different parameters like the final carbonisation temperature, the heating rate to reach the final temperature, the holding time at the final temperature, and the number of steps during which the carbonisation process was carried out. Multi-response optimisation was performed using grey rational statistical analysis in order to optimise settings to achieve higher values of electrical conductivity and electromagnetic shielding while maintaining the surface area at a moderate level, as a rise in the surface area adversely affects the surface resistivity and electromagnetic shielding capability of activated carbon fibre. The outcomes of this study showed that an increase in carbonisation temperature resulted in not only an increase in parallel orientation but also a reduction in the space among the basal planes of carbon, which ultimately led to a more compact structure of the AC web, thus causing a reduction in resistivity from 136.41 Ωmm to 0.26 Ωmm. This reduction in resistivity ultimately brought about an increase in electromagnetic shielding from 2.1 dB to 81.33 dB. There was not much difference in surface resistivity when the heating rate was slow, but it resulted in significantly less yield and poor flexibility of the AC web. However, a fused, rigid and brittle web was produced at a high heating rate due to the sudden rise in temperature during carbonisation. The AC web developed in three steps gave better conductivity and shielding because of improved stabilisation, which helped in the development of a flexible web during carbonisation. The surface resistivity was decreased from 1.19 Ωmm to 0.26 Ωmm, and correspondingly electromagnetic shielding increased from 80.1 dB to 81.33 dB at 1200 °C with a holding time of 60 minutes and heating rate of 300 °C/h in the three step approach. From the above results, it was concluded that the AC web prepared at the optimum settings not only resulted in good electrical conductivity and electromagnetic shielding but also provided good flexibility and yield, which can be effectively employed in apparels as inter lining material for electromagnetic shielding purposes.


## Acknowledgements

*This work was supported by the Higher Education Commission, Pakistan: [Grant Number 21-2137/SRGP/R&D/HEC/2018].*


## References


1. Šafářová V, Militký J. Electromagnetic Shielding Properties of Woven Fabrics made from High-Performance Fibers. *Textile Research Journal* 2014; 84(12): 1255-67.
2. Šafářová V, Tunák M, Militký J. Prediction of Hybrid Woven Fabric Electromagnetic Shielding Effectiveness. *Textile Research Journal* 2015; 85(7): 673-86.
3. Šafářová V, Militký J. Comparison of Methods for Evaluating the Shielding Effectiveness of Textiles. *Vlakna a Textil* 2012; 19: 50-6.
4. Chung D. Electromagnetic Interference Shielding Effectiveness of Carbon Materials. *Carbon* 2001; 39(2): 279-85.
5. Cao M-S, Wang X-X, Cao W-Q, Yuan J. Ultrathin Graphene: Electrical Properties and Highly Efficient Electromagnetic Interference Shielding. *Journal of Materials Chemistry* C. 2015; 3(26): 6589-99.
6. Sano E, Akiba E. Electromagnetic Absorbing Materials using Nonwoven Fabrics Coated With Multi-Walled Carbon Nanotubes. *Carbon* 2014; 78: 463-8.
7. Rubežienė V, Baltušnikaitė J, Varnaitė-Žuravliova S, Sankauskaitė A, Abraitienė A, Matuzas J. Development and Investigation of Electromagnetic Shielding Fabrics with Different Electrically Conductive Additives. *Journal of Electrostatics* 2015;75: 90-8.
8. Tian M, Du M, Qu L, Chen S, Zhu S, Han G. Electromagnetic Interference Shielding Cotton Fabrics with High Electrical Conductivity and Electrical Heating Behavior via Layer-By-Layer Self-Assembly Route. *RSC Advances* 2017; 7(68): 42641-52.
9. Neruda M, Vojtech L. Electromagnetic Shielding Effectiveness of Woven Fabrics with High Electrical Conductivity: Complete Derivation and Verification of Analytical Model. *Materials* 2018; 11(9): 1657.
10. Cao M-S, Yang J, Song W-L, Zhang D-Q, Wen B, Jin H-B, et al. Ferroferric Oxide/Multiwalled Carbon Nanotube Vs Polyaniline/Ferroferric Oxide/Multiwalled Carbon Nanotube Multiheterostructures for Highly Effective Microwave Absorption. *ACS Applied Materials & Interfaces* 2012; 4(12): 6949-56.
11. Li Y, Shen B, Pei X, Zhang Y, Yi D, Zhai W, et al. Ultrathin Carbon Foams for Effective Electromagnetic Interference Shielding. *Carbon* 2016; 100: 375-85.
12. Chen JY. Activated Carbon Fiber and Textiles: Woodhead Publishing; 2016.
13. Lee J, Lee B, Kim B, Park M, Lee D, Kuk I, et al. The Effect of Carbonization Temperature of PAN Fiber on the Properties of Activated Carbon Fiber Composites. *Carbon* 1997; 35(10-11): 1479-84.
14. Morawski A, Kałucki K, Nakashima M, Inagaki M. Modified Carbonization of Polyacrylonitrile by Incorporation of Fecl2 and Fe (NO3) 3 – Pore Structure. *Carbon* 1994; 32(8): 1457-61.
15. Zhang Y, Wang M, He F, Zhang B. Mesopore Development in PAN-ACF Resulting from Non-Metal Additives. *Journal of Materials Science* 1997; 32(22): 6009-13.
16. Stoeckli F, Centeno TA, Fuertes A, Muniz J. Porous Structure of Polyarylamide -Based Activated Carbon Fibres. *Carbon* 1996; 34(10): 1201-6.
17. Daley M, Mangun C, DeBarrb J, Riha S, Lizzio A, Donnals G, et al. Adsorption of SO2 Onto Oxidized and Heat-Treated Activated Carbon Fibers (ACFs). *Carbon* 1997; 35(3): 411-7.
18. Mangun C, Daley M, Braatz R, Economy J. Effect of Pore Size on Adsorption of Hydrocarbons in Phenolic-Based Activated Carbon Fibers. *Carbon* 1998; 36(1-2): 123-9.
19. Kumar K, Saxena R, Kothari R, Suri D, Kaushik N. Correlation between Adsorption and X-Ray Diffraction Studies on Viscose Rayon Based Activated Carbon Cloth. *Carbon* (New York, NY) 1997; 35(12): 1842-4.
20. Ahmad N, Kamal S, Raza ZA, Hussain T, Anwar F. Multi-Response Optimization in the Development of Oleo-Hydrophobic Cotton Fabric Using Taguchi Based Grey Relational Analysis. Applied Surface Science 2016; 367: 370-81.
21. Siqueira G, Abdillahi H, Bras J, Dufresne A. High Reinforcing Capability Cellulose Nanocrystals Extracted From Syngonanthus Nitens (Capim Dourado). *Cellulose* 2010; 17(2): 289-98.
22. Naeem S, Baheti V, Militky J, Wiener J, Behera P, Ashraf A. Sorption Properties of Iron Impregnated Activated Carbon Web for Removal of Methylene Blue from Aqueous Media. *Fibers and Polymers* 2016; 17(8): 1245-55.
23. Naeem S, Baheti V, Tunakova V, Militky J, Karthik D, Tomkova B. Development

of Porous and Electrically Conductive Activated Carbon Web for Effective EMI Shielding Applications. *Carbon* 2017; 111: 439-47.
24. Baheti V, Naeem S, Militky J, Okrasa M, Tomkova B. Optimized Preparation of Activated Carbon Nanoparticles from Acrylic Fibrous Wastes. *Fibers and Polymers* 2015; 16(10): 2193-201.
25. Wen B, Cao M-S, Hou Z-L, Song W-L, Zhang L, Lu M-M, et al. Temperature Dependent Microwave Attenuation Behavior For Carbon-Nanotube/Silica Composites. *Carbon* 2013; 65: 124-39.
26. Song W-L, Cao M-S, Hou Z-L, Fang X-Y, Shi X-L, Yuan J. High Dielectric Loss and its Monotonic Dependence of Conducting-Dominated Multiwalled Carbon Nanotubes/Silica Nanocomposite on Temperature Ranging from 373 To 873 K In X-Band. *Applied Physics Letters* 2009; 94(23): 233110.
27. Arjmand M, Chizari K, Krause B, Pötschke P, Sundararaj U. Effect of Synthesis Catalyst on Structure of Nitrogen-Doped Carbon Nanotubes and Electrical Conductivity and Electromagnetic Interference Shielding of their Polymeric Nanocomposites. *Carbon* 2016; 98: 358-72.
28. Zou L, Lan C, Li X, Zhang S, Qiu Y, Ma Y. Superhydrophobization of Cotton Fabric with Multiwalled Carbon Nanotubes for Durable Electromagnetic Interference Shielding. *Fibers and Polymers* 2015; 16(10): 2158-64.
29. Simayee M, Montazer M. A Protective Polyester Fabric with Magnetic Properties using Mixture of Carbonyl Iron and Nano Carbon Black Along with Aluminium Sputtering. *Journal of Industrial Textiles* 2018; 47(5): 674-85.
30. Bonaldi RR, Siores E, Shah T. Characterization of Electromagnetic Shielding Fabrics Obtained from Carbon Nanotube Composite Coatings. *Synthetic Metals* 2014; 187:1-8.
31. Gupta K, Abbas S, Abhyankar A. Carbon Black/Polyurethane Nanocomposite-Coated Fabric for Microwave Attenuation in X & Ku-Band (8-18 Ghz) Frequency Range. *Journal of Industrial Textiles* 2016; 46(2): 510-29.
32. Arjmand M, Sundararaj U. Electromagnetic Interference Shielding of Nitrogen-Doped and Undoped Carbon Nanotube/Polyvinylidene Fluoride Nanocomposites: A Comparative Study. *Composites Science and Technology* 2015; 118: 257-63.
33. Cao M-S, Song W-L, Hou Z-L, Wen B, Yuan J. The Effects of Temperature and Frequency on the Dielectric Properties, Electromagnetic Interference Shielding and Microwave-Absorption of Short Carbon Fiber/Silica Composites. *Carbon* 2010; 48(3): 788-96.
34. Bansal RC, Goyal M. *Activated carbon adsorption: CRC press*; 2005.

***Received 07.01.2020 Reviewed 21.05.2020***